Mechanics of Advanced Composite Structures 9 (2022) 335 – 348

Semnan University

Mechanics of Advanced Composite Structures

journal homepage: http://MACS.journals.semnan.ac.ir

Effect of Elastically Restrained Edges on Free Transverse Vibration of Functionally Graded Porous Rectangular Plate

Y. Kumar *

Department of Mathematics, Government Girls Degree College, Behat- 247121, India

KEYWORDS

Functionally graded;
Porous rectangular;
Restrained;
Physical neutral surface;
Rayleigh-Ritz.

ABSTRACT

In this paper, the author studied free transverse vibration of a thin isotropic simply-supported functionally graded (FG) rectangular plate with porosity effect based on classical plate theory. The plate is considered to be elastically restrained against rotation. It is assumed that the material properties of the graded plate are porosity-dependent. An even porosity distribution is considered for analysis purposes. Due to the asymmetry of material in the thickness direction, the neutral surface is not the same as the geometrical mid-plane of the plate. The concept of the physical neutral surface of the FG plate along with classical plate theory is used to formulate the problem. Hence, the physical neutral surface is taken as the reference plane. The first three dimensionless frequencies of the plate are obtained using the Rayleigh-Ritz method. Boundary characteristic orthogonal polynomials (eigenfunctions), generated using the Gram-Schmidt process, are used in the Rayleigh-Ritz method. A parametric study shows that porosity and material distribution parameters have remarkable effects on the free vibration response of the plate. Results are compared with those of simply-supported FG plates.

1. Introduction

Functionally graded materials, generally made of ceramic and metal, are nonhomogeneous materials in which material properties vary continuously in appropriate directions. Free transverse vibration analysis of FG rectangular plates has gained attention of many researchers. A few papers about free vibration of FG plates have appeared in the literature and are summarized as follows: Dynamic response of initially stressed FG rectangular thin plates resting on elastic foundation has been studied by Yang and Shen [1]. Abrate [2] studied free vibrations, buckling, and static deflections of FG rectangular plates. He concluded that the natural frequencies of FG plates are proportional to those of homogeneous isotropic plates. Ferreira et. al. [3] computed natural frequencies of square FG plates employing the asymmetric collocation method. Zhao et. al. [4] presented the mechanical and thermal buckling analysis of FG rectangular plates using first-order shear deformation theory and the element-free kp-Ritz method. Talha and Singh [5] studied static and free vibration of FGM plates using higher order shear deformation theory in conjunction with FEM. Janghorban and Zareb [6] investigated the thermal effect on free vibration of FG arbitrary straight-sided plates with circular and non-circular cut-outs. Ghannadpour et. al. [7] used the finite strip method to analyse the buckling behaviour of FG rectangular plates under thermal loading. The plates were subjected to distributed impulsive loads. Thermal buckling of FG skew and trapezoidal plates has been investigated by Jaberzadeh et. al. [8] using the element-free Galerkin method. Baferani et. al. [9] investigated free vibration of FG rectangular plates based on first-order shear deformation theory. Chakraverty and Pradhan [10-11] investigated free vibration of thin FG rectangular plates incorporating the effects of Winkler foundation and thermal environment using the Rayleigh-Ritz method. Pradhan and Chakraverty [12] dealt with static analysis of thin FG rectangular plates under mechanical load using the Rayleigh-Ritz method. Khorshidi and Bakhsheshy [13]

* Corresponding author. Tel.: +91-9997125309
E-mail address: yaju_saini@yahoo.com

DOI: 10.22075/macs.2022.26866.1393
Received 2022-04-14; Received in revised form 2022-07-04; Accepted 2022-08-27.

investigated the vibration analysis of FG rectangular plates partially in contact with a fluid. Pham [14] developed an analytical solution to investigate the thermal buckling of imperfect rectangular plates with FG coating under uniform temperature rise. Atmane et. al. [15] studied thermal buckling of a simply supported sigmoid FG rectangular plate employing first-order shear deformation theory. Lee et. al. [16] presented a thermal buckling analysis of FG rectangular plates based on the neutral surface of a structure. Kumar et. al. [17] investigated free vibration of thin FG rectangular plates using the dynamic stiffness method.

The materials having pores are termed as porous materials. The application of these materials in the aeronautical industry, energy absorbing systems, sound absorbers, insulating materials, heat exchangers, construction materials, and electromagnetic shielding has necessitated the study of different behaviors of structures made of porous materials in recent years [18]. A significant number of works dealing with the static, bending, vibration, and buckling problems of porous beams and plates are reviewed as follows: Theodorakopoulos and Beskos [19] studied flexural vibration of thin, rectangular, simply-supported, and fluid-saturated porous plates. Leclaire et. al. [20] presented a simple model of the transverse vibration of a thin rectangular porous plate saturated by a fluid. The vibration of a clamped rectangular porous plate using Galerkin's variational method has been presented by Leclaire et. al. [21]. Vibration analysis of porous FG beams was presented by Wattanasakulpong and Ungbhakorn [22]. Razaei and Saidi [23] presented an exact solution for the vibration of rectangular porous plates using Reddy's third-order shear deformation theory. Mojahedin et. al. [24] studied the buckling of FG circular porous plates using the energy method based on higher-order shear deformation theory. Chen et. al. [25] presented free and forced vibration of FG porous beams with different kinds of porosity distributions. Ebrahimi and Habibi [26] presented a finite element formulation for deflection and vibration of FG porous plates based on higher-order shear deformation theory. Mechab et. al. [27-28] studied free vibration/probabilistic analysis of FG nanoplate with porosities resting on Winkler-Pasternak elastic foundation. Jahwari and Naguib [29] presented an analysis of FG viscoelastic porous structure with a higher order plate theory. Barati et. al. [30] used a refined four-variable theory to study the buckling of FG piezoelectric porous plates resting on an elastic foundation. Barati and Zenkour [31] explored the electro-thermo-mechanical vibrational behavior of FG piezoelectric plates with porosity using a refined four-variable plate theory. Mouaici et. al. [32] used hyperbolic shear deformation theory to examine the effect of porosity on the vibration of non-homogeneous plates. Ebrahimi and Jafari [33] presented an analytical solution to study the buckling characteristics of porous magneto-electro-elastic FG plates. In a series of papers, Rezaei and co-workers [34-40] studied the free vibration and buckling behavior of porous plates employing various plate models. Kamranfard et. al. [41] presented an analytical solution for vibration and buckling of porous annular sector plates under in-plane uniform compressive loads. Şimşek and Aydın [42] used a modified couple stress theory to study the forced vibration of FG microplates with porosity effects. Akbas [43] dealt with free vibration and static bending of simply supported FG plates with porosity effect incorporating first-order shear deformation theory. Barati and co-workers [44-47] have presented vibration analysis of smart/nano FG porous plates using a refined four-variable theory. Ali et. al. [48] studied free vibration of the embedded porous plate using higher order shear deformation theory. Wang and Zu [49-51] studied free/forced vibration of FG rectangular porous plates with different complicating effects. Wang and Yang [52] investigated the nonlinear vibration of moving FG plates in contact with liquid and containing porosities. Electro-mechanical vibration analysis of FG piezoelectric porous plates in the translation state has been presented by Wang [53]. Kiran et. al. [54] studied the effect of porosity on the structural behavior of skew functionally graded magneto-electro-elastic plates. Free vibration analysis of saturated porous circular plates made of FG material integrated with a piezoelectric actuator is presented by Arshid and Khorshidvand [55] using the differential quadrature method. Arani et. al. [56] dealt with the dynamic analysis of rectangular porous plates resting on the Pasternak foundation using high-order shear deformation theory. Gupta and Talha [57] presented the influence of porosity on flexural and free vibration of FG plates in a thermal environment based on non-polynomial higher-order shear and normal deformation theory. Zhao et. al. [58] studied free vibration of functionally graded porous rectangular plates by means of an improved Fourier series method considering three types of porosity distributions. Daikh and Zenkour [59] obtained a Navier solution of free vibration and mechanical buckling of porous functionally graded sandwich plates using higher-order shear deformation theory. Du et. al. [60] performed a free vibration analysis of rectangular plates with three types of porosity distributions using the Rayleigh-Ritz method based on first-order shear deformation theory. Rjoub and Alshatnawi [61] predicted the

natural frequencies of a simply-supported functionally graded porous cracked plate using the Artificial Neural Network technique. Bansal et. al. [62] provided Navier solution and FEM-based solution of vibration of porous functionally graded plates with geometric discontinuities and partial supports based on the refined exponential shear deformation theory. Tran et. al. [63] presented static and free vibration of functionally graded porous plates using an edge-based smoothed finite element method. Chai and Wang [64] investigated traveling wave vibration of spinning graphene platelets reinforced porous joined conical-cylindrical shells using the power series method.

An up-to-date review of works pertaining to the application of the Rayleigh-Ritz method in vibration analysis of structural elements is given by Kumar [65] and Pablo et. al. [66]. In their two papers, Wang and co-workers [67-68] used the Rayleigh-Ritz method to analyze the vibration of longitudinally moving plate submerged in an infinite liquid domain and that of FG cylindrical shells with porosities.

In some engineering problems, the boundary conditions along the edges of the plate are assumed to be either clamped or simply supported. But the actual boundary conditions tend to be in between these two limiting cases. To achieve these boundary conditions, analysis is done by modeling the edge conditions as a collection of elastic springs whose combined effect could vary from zero to infinity. Very few researchers (Laura and Grossi [69], Okan [70], Kumar [71], Zhang et. al. [72], He et. al. [73]) have considered the effect of elastically restrained edges against rotation on the vibration of plates.

The objective of this work is to study the free transverse vibration of a thin isotropic FG rectangular plate with even porosity distribution. The plate is simply-supported and elastically restrained against rotation along the edges. Material properties of the plate, continuously varying in the thickness direction, are assumed to be dependent on porosity. The Rayleigh-Ritz method incorporating boundary characteristic orthogonal polynomials as eigenfunctions is used to obtain the first three natural frequencies and mode shapes.

2. Formulation of the problem

Let us consider a thin isotropic FG elastically restrained against a rotation rectangular plate made of porous material with length '*a*' taken in the x direction, breadth '*b*' in the y direction and thickness '*h*' in z direction as shown in Fig. 1. The top surface (*h/2*) is ceramic rich while bottom surface (*-h/2*) is metal rich.

The physical neutral surface does not coincide with the geometrical mid-plane of the plate. The distance between the geometrical mid-plane and the physical neutral surface is considered to be z_0. There exists uniformly distributed (even) porosity in the plate. In this model, porosity spreads uniformly through the thickness direction.

The strains are defined as:

$$\varepsilon_x = -(z - z_0)\frac{\partial^2 w}{\partial x^2},$$
$$\varepsilon_y = -(z - z_0)\frac{\partial^2 w}{\partial y^2}, \quad (1)$$
$$\varepsilon_{xy} = -2(z - z_0)\frac{\partial^2 w}{\partial x \partial y}.$$

According to Hook's law

$$\sigma_x = \frac{E(z)}{1-\upsilon^2}(\varepsilon_x + \upsilon\varepsilon_y),$$
$$\sigma_y = \frac{E(z)}{1-\upsilon^2}(\upsilon\varepsilon_x + \varepsilon_y), \quad (2)$$
$$\sigma_{xy} = \frac{E(z)}{2(1+\upsilon)}\varepsilon_{xy}.$$

Using relation (1) in (2), we obtain

$$\sigma_x = -(z - z_0)\frac{E(z)}{1-\upsilon^2}\left(\frac{\partial^2 w}{\partial x^2} + \upsilon\frac{\partial^2 w}{\partial y^2}\right),$$
$$\sigma_y = -(z - z_0)\frac{E(z)}{1-\upsilon^2}\left(\upsilon\frac{\partial^2 w}{\partial x^2} + \frac{\partial^2 w}{\partial y^2}\right), \quad (3)$$
$$\sigma_{xy} = -(z - z_0)\frac{E(z)}{(1+\upsilon)}\frac{\partial^2 w}{\partial x\,\partial y}.$$

The expression for the strain energy is

$$V = \frac{1}{2}\int_0^a\int_0^b\int_{-\frac{h}{2}}^{\frac{h}{2}}\left(\begin{matrix}\sigma_x\varepsilon_x + \sigma_y\varepsilon_y \\ + \sigma_{xy}\varepsilon_{xy}\end{matrix}\right)\,dx\,dy\,dz. \quad (4)$$

Using relations (1) and (3) in (4), strain energy becomes

$$V = \frac{1}{2(1-\upsilon^2)}\int_0^a\int_0^b\int_{-\frac{h}{2}}^{\frac{h}{2}}(z-z_0)^2 E(z)\left[\begin{matrix}\left(\frac{\partial^2 w}{\partial x^2}\right)^2 \\ + 2\upsilon\frac{\partial^2 w}{\partial x^2}\frac{\partial^2 w}{\partial y^2} \\ + 2(1-\upsilon)\left(\frac{\partial^2 w}{\partial x\partial y}\right)^2 \\ + \left(\frac{\partial^2 w}{\partial y^2}\right)^2\end{matrix}\right]dxdydz. \quad (5)$$

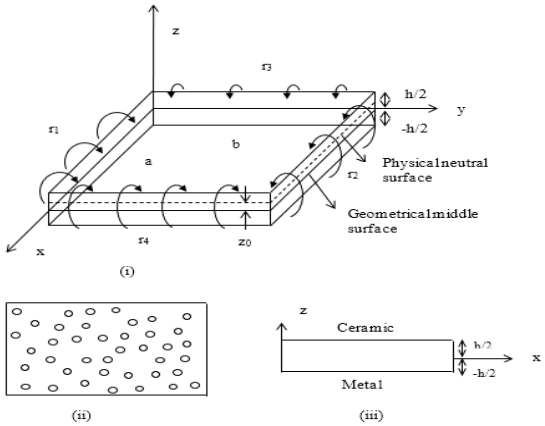

Fig. 1. (i) FG porous elastically restrained rectangular plate with physical neutral surface and geometrical middle surface (ii) plate with even porosity (iii) cross-section of the plate

The kinetic energy of the plate is given as

$$T = \frac{1}{2}\int_0^a \int_0^b \int_{-h/2}^{h/2} \rho(z)\left(\frac{\partial w}{\partial t}\right)^2 dx\, dy\, dz, \qquad (6)$$

where $w(x,y,t)$ is the displacement, $E(z)$ is Young's modulus, $\rho(z)$ is the density, υ is the Poisson's ratio, the subscript following a variable denotes differentiation of the variable w.r.to the subscript following it, and t is the time.

The effective material properties viz. Young's modulus and density are assumed to be graded in the thickness direction according to the power law (Wattanasakulpong and Ungbhakorn [22]) as follows:

$$E(z) = (E_c - E_m)\left(\frac{1}{2} + \frac{z}{h}\right)^g + E_m - (E_c + E_m)\frac{k}{2}, \qquad (7)$$

$$\rho(z) = (\rho_c - \rho_m)\left(\frac{1}{2} + \frac{z}{h}\right)^g + \rho_m - (\rho_c + \rho_m)\frac{k}{2}, \qquad (8)$$

where E_c, E_m are young's moduli of ceramic and metal; ρ_c, ρ_m are densities of ceramic and metal; g is the non-negative volume fraction index which describes the material distribution across the thickness of the plate and $k\,(k << 1)$ is porosity volume fraction. The value of k equal to 0 corresponds to the perfect FG plate. The plate becomes isotropic homogeneous if either $g = 0$ (fully ceramic) or $g = \infty$ (fully metal).

For harmonic solution, the displacement $w(x,y,t)$ is assumed to be

$$w(x,y,t) = \overline{W}(x,y)\, e^{i\omega t}, \qquad (9)$$

where ω is the circular frequency, $\overline{W}(x,y)$ represents the maximum transverse displacement at the point (x,y) and $i = \sqrt{-1}$.

Using relations (7), (8), and (9), the expressions for maximum strain energy and kinetic energy of the plate become

$$V_{\max} = \frac{1}{2} D_{eff} \int_0^a \int_0^b [\overline{W}_{xx}^{\,2} + 2\upsilon \overline{W}_{xx}\overline{W}_{yy} + 2(1-\upsilon)\overline{W}_{xy}^{\,2} + \overline{W}_{yy}^{\,2}]\, dx\, dy \qquad (10)$$

and

$$T_{\max} = \frac{\omega^2 \rho_{eff}\, h}{2} \int_0^a \int_0^b \overline{W}^2\, dx\, dy, \qquad (11)$$

where

$$D_{eff} = \int_{-h/2}^{h/2} (z - z_0)^2 \frac{E(z)}{(1-\upsilon^2)} dz \qquad (12)$$

$$= \frac{12 D_c}{\frac{E_c}{E_m}} \begin{bmatrix} \frac{3\frac{E_c}{E_m}(g^2+g+2) + (g^3+3g^2+8g)}{12(g+1)(g+2)(g+3)} \\ -\left(\frac{z_0}{h}\right)\frac{g\left(\frac{E_c}{E_m}-1\right)}{(g+1)(g+2)} \\ +\left(\frac{z_0}{h}\right)^2 \frac{\left(\frac{E_c}{E_m}+g\right)}{(g+1)} - \frac{1}{12}\left(\frac{E_c}{E_m}+1\right)\frac{k}{2} \\ -\left(\frac{z_0}{h}\right)^2\left(\frac{E_c}{E_m}+1\right)\frac{k}{2} \end{bmatrix}, \qquad (13)$$

$$\rho_{eff} = \frac{1}{h}\int_{-h/2}^{h/2} \rho(z)dz = \rho_c \begin{pmatrix} \left\{\frac{2-(g+1)k}{2(g+1)}\right\} \\ +\left\{\frac{2g-(g+1)k}{2(g+1)}\right\}\frac{\rho_m}{\rho_c} \end{pmatrix}, \qquad (14)$$

$$z_0 = \frac{\int_{-h/2}^{h/2} zE(z)dz}{\int_{-h/2}^{h/2} E(z)dz} = \frac{hg\left(\frac{E_c}{E_m}-1\right)}{2(g+2)\left(\left(\frac{E_c}{E_m}-1\right)+(g+1)\left\{1-\left(\frac{E_c}{E_m}+1\right)\frac{k}{2}\right\}\right)} \qquad (15)$$

The maximum strain energy (Warburton and S.L. Edney [74]) associated with the rotational restraints in the edges is given by

$$U_{\max} = \frac{1}{2}[r_1\int_0^a \overline{W}_y^{\,2}(x,0)\,dx + r_2\int_0^a \overline{W}_y^{\,2}(x,b)\,dx + r_3\int_0^b \overline{W}_x^{\,2}(0,y)\,dy + r_4\int_0^b \overline{W}_x^{\,2}(a,y)\,dy], \qquad (16)$$

where $r_i (i = 1,2,3,4)$ are the rotational spring constants.

Introducing the non-dimensional variables $X = x/a,\ Y = y/b,\ W = \overline{W}/a$ together with

$$W(X,Y) = \sum_{j=1}^{N} d_j \hat{\phi}_j(X,Y), \qquad (17)$$

We obtain the standard eigenvalue problem as follows:

$$\sum_{j=1}^{N}(a_{ij} - \Omega^2\delta_{ij})\, d_j = 0, i = 1,2,3,\ldots\ldots,N, \qquad (18)$$

where N is the order of approximation to get the desired accuracy, $\hat{\phi}_j$ are orthonormal polynomials, d_j are unknowns,

$$a_{ij}=\frac{D^*_{eff}}{\rho^*_{eff}}\int_0^1\int_0^1\begin{Bmatrix}\hat{\phi}_i^{XX}\hat{\phi}_j^{XX}\\+\upsilon\mu^2\begin{pmatrix}\hat{\phi}_i^{XX}\hat{\phi}_j^{YY}\\+\hat{\phi}_j^{XX}\hat{\phi}_i^{YY}\end{pmatrix}\\+2(1-\upsilon)\mu^2\hat{\phi}_i^{XY}\hat{\phi}_j^{XY}\\+\mu^4\hat{\phi}_i^{YY}\hat{\phi}_j^{YY}\end{Bmatrix}dXdY+ \quad (19)$$

$$\frac{1}{\rho^*_{eff}}\begin{bmatrix}R_1\mu^3\int_0^1\left[\hat{\phi}_i^{Y}\hat{\phi}_j^{Y}\right]_{Y=0}dX+R_2\mu^3\int_0^1\left[\hat{\phi}_i^{Y}\hat{\phi}_j^{Y}\right]_{Y=1}dX\\+R_3\mu\int_0^1\left[\hat{\phi}_i^{X}\hat{\phi}_j^{X}\right]_{X=0}dY+R_4\mu\int_0^1\left[\hat{\phi}_i^{X}\hat{\phi}_j^{X}\right]_{X=1}dY\end{bmatrix},$$

$$D^*_{eff}=\frac{D_{eff}}{D_c},\ \rho^*_{eff}=\frac{\rho_{eff}}{\rho_c},$$

$$R_1=\frac{r_1a}{D_c},R_2=\frac{r_2a}{D_c},R_3=\frac{r_3b}{D_c},R_4=\frac{r_4b}{D_c},$$

$$\mu=\frac{a}{b},\ \Omega=\omega a^2\sqrt{\frac{\rho_c h}{D_c}},\ \ D_c=\frac{E_c h^3}{12(1-\upsilon^2)},$$

$$\delta_{ij}=\begin{cases}1, & if\ \ i=j\\0, & if\ \ i\neq j\end{cases},$$

and Ω is the frequency parameter.

The orthonormal polynomials $\hat{\phi}_k$ are generated using the Gram-Schmidt process (Singh and Chakraverty [75]).

3. Results

In this modal analysis, a plate made of functionally graded material (Aluminium/ Alumina, i.e., Al/Al_2O_3) is considered. Here, the symbol R_{ijkl} is used for $R_i=R_j=R_k=R_l$ and R_{ij} represents $R_i=R_j, R_k=R_l=0.$ The following values of material coefficients (Talha and Singh [5]) for the FG plate and other parameters are taken:

$$E_m=70GPa,\ \ E_c=380GPa, \rho_m=2707\,kg/m^3,$$

$$\rho_c=3800\,kg/m^3; k=0.1,0.2,0.3;$$

$$g=1,2,3,4,5;\ \mu=0.5,1.0,1.5,2.0;$$

$$R_{1234}=1,10,10^2,10^3,10^4,10^5,10^6,10^7;$$

$$N=26.$$

We also assume that the Poisson's ratio υ remains constant along the thickness direction as the plate is considered to be thin. The first three values of the frequency parameter Ω have been calculated from the standard eigenvalue problem given by (18). For this purpose, a computer program has been developed by the author in C++. Table 1 shows the convergence of frequency parameter Ω with increasing N. To achieve an accuracy of four decimal places, the value of N has been fixed as 26. A comparison of frequencies of simply-supported isotropic FG rectangular/square plates is shown in Table 2. The results are in good agreement with those available in the literature. The results have been reported in Tables (3-5) and Figs. (2-7).

Table 1. Convergence of first three values of frequency parameter Ω of FG porous plate with increasing value of N

				N			
k	Mode	10	15	20	24	25	26
				$\mu=1.0, g=5,\ R_{1234}=1000$			
	I	89.7801	10.2914	10.2914	10.2914	10.2914	10.2914
0.3	II	179.1420	179.1420	21.2307	21.2264	21.2264	21.2264
	III	913.5480	179.1420	21.2390	21.2264	21.2264	21.2264
				$\mu=1.0, g=5,\ R_{1234}=10000000$			
	I	8923.51	10.2931	10.2931	10.2931	10.2931	10.2931
0.3	II	17796.3	17796.3	21.2429	21.2429	21.2429	21.2429
	III	91336.8	17796.3	21.2430	21.2429	21.2429	21.2429
				$\mu=2.0, g=2,\ R_{1234}=10000000$			
	I	16078	64.7397	64.7397	64.7397	64.6713	64.6713
0.1	II	30095.9	29615.5	83.7024	83.7024	83.7024	83.7024
	III	107816	30095.9	171.346	171.3450	119.9290	119.9290
				$\mu=2.0, g=2,\ R_{1234}=0$			
	I	29.5262	29.5218	29.5160	29.5160	29.5160	29.5160
0.2	II	47.3251	47.3251	47.2301	47.2262	47.2262	47.2262
	III	99.1221	77.5665	77.5665	76.8723	76.7577	76.7577
				$\mu=1.0, g=5,\ R_{12}=10000000$			
	I	15.2531	15.0241	15.0241	15.0238	15.0238	15.0238
0.2	II	32.9505	32.9504	28.4808	28.4808	28.4808	28.4808
	III	36.5462	36.5462	35.9856	35.9856	35.9856	35.9856

Table 2. Comparison of frequency parameter Ω of simply-supported FG plate

g	μ	Reference	Mode I	Mode II	Mode III
0	0.4	Leissa [76]	11.4487	16.1862	24.0818
		Present	11.4487	16.1863	24.2984
	1.0	Leissa [76]	19.7392	49.3480	49.3480
		Present	19.7392	49.3490	49.3490
	1.5	Leissa [76]	32.0762	61.6850	98.6960
		Present	32.0762	61.6860	98.6982
0.2	1.0	Kumar et. al. [17]	18.3177	45.7942	45.7942
		Present	18.3177	45.7951	45.7951
1.0	0.5	Kumar et. al. [17]	9.4131	15.0610	24.4741
		Present	9.4131	15.0612	24.7371
	1.0	Kumar et. al. [17]	15.0610	37.6524	-
		Present	15.0610	37.6531	-
	2.0	Kumar et. al. [17]	37.652	60.244	97.896
		Present	37.6524	60.2447	97.9168
5.0	1.0	Kumar et. al. [17]	12.9831	32.4578	32.4578
		Present	12.9831	32.4584	32.4584

Table 3. First three values of frequency parameter Ω of FG porous plate for $R_{1234}=100$

		g					
		0	1	2	3	4	5
k	Mode	$\mu=0.5$					
	I	20.3576	16.7595	15.5579	15.1744	15.0228	14.9330
0.0	II	28.1742	22.5141	20.7440	20.1829	19.9590	19.8262
	III	45.3146	37.7248	35.6836	35.1296	34.9489	34.8525
	I	20.8079	16.6007	14.9632	14.3858	14.1615	14.0502
0.1	II	28.7066	22.1958	19.8414	19.0234	18.7051	18.5464
	III	46.2599	37.7577	35.1488	34.3706	34.1258	34.0306
	I	21.3262	16.2883	13.8835	12.8726	12.4421	12.2443
0.2	II	29.3263	21.6684	18.2965	16.9092	16.3217	16.0518
	III	47.3702	37.6793	34.1196	32.8494	32.3928	31.9499
	I	21.9326	15.6980	11.6935	9.3033	7.8542	6.9551
0.3	II	30.0596	20.7689	15.3005	12.1211	10.2133	9.0352
	III	48.6954	37.3800	30.5239	24.3207	20.5589	18.2235
		$\mu=1.0$					
	I	34.6795	26.9424	24.5964	23.8533	23.5532	23.3746
0.0	II	70.9287	55.1290	50.3468	48.8330	48.2222	47.8587
	III	70.9287	55.1290	50.3468	48.8330	48.2222	47.8587
	I	35.2494	26.4107	23.3518	22.3010	21.8902	21.6839
0.1	II	72.0935	54.0525	47.8166	45.6753	44.8387	44.4189
	III	72.0935	54.0525	47.8166	45.6753	44.8387	44.4189
	I	35.9161	25.6153	21.3390	19.6197	18.8964	18.5636
0.2	II	73.4572	52.4395	43.7197	40.2136	38.7386	38.0605
	III	73.4572	52.4395	43.7197	40.2136	38.7386	38.0605
	I	36.7098	24.3647	17.6371	13.8647	11.6389	10.2761
0.3	II	75.0818	49.8999	36.1736	28.4688	23.9184	21.1299
	III	75.0818	49.8999	36.1736	28.4688	23.9184	21.1299
		$\mu=2.0$					
	I	81.4036	67.0071	62.2002	60.6664	60.0599	59.7007
0.0	II	112.6970	90.0566	82.9760	80.7316	79.8361	79.3049
	III	167.1160	130.9970	120.0990	116.6610	115.2840	114.4660
	I	83.2031	66.3703	59.8209	57.5116	56.6146	56.1699
0.1	II	114.8260	88.7832	79.3657	76.0936	74.8202	74.1856
	III	169.9390	128.7410	114.4610	109.5510	107.6400	106.6850
	I	85.2746	65.1195	55.5028	51.4611	49.7399	48.9492
0.2	II	117.3050	86.6735	73.1861	67.6369	65.2870	64.2072
	III	173.2520	125.2630	105.1450	96.9921	93.5559	91.9784
	I	87.6980	62.7578	46.7478	37.1944	31.4035	27.8106
0.3	II	120.2380	83.0756	61.2021	48.4844	40.8531	36.1407
	III	177.2070	119.6390	87.5955	69.2985	58.3839	51.6567

Table 4. First three values of frequency parameter Ω of FG porous plate for $R_{1234}=10000000$

		g					
		0	1	2	3	4	5
k	Mode			$\mu=0.5$			
	I	24.6096	18.7771	17.0717	16.5339	16.3162	16.1866
0.0	II	31.8669	24.3144	22.1060	21.4097	21.1278	20.9599
	III	65.2334	49.7732	45.2527	43.8272	43.2501	42.9065
	I	24.9625	18.3586	16.1601	15.4106	15.1175	14.9701
0.1	II	32.3237	23.7724	20.9256	19.9551	19.5756	19.3847
	III	66.1687	48.6639	42.8363	40.8496	40.0728	39.6820
	I	25.3817	17.7570	14.7195	13.5109	13.0037	12.7705
0.2	II	32.8666	22.9934	19.0602	17.4952	16.8385	16.5364
	III	67.2800	47.0693	39.0177	35.8139	34.4697	33.8514
	I	25.8882	16.8410	12.1213	9.5079	7.9736	7.0364
0.3	II	33.5225	21.8074	15.6958	12.3118	10.3250	9.1114
	III	68.6226	44.6413	32.1304	25.2031	21.1361	18.6517
				$\mu=1.0$			
	I	36.0000	27.4679	24.9732	24.1865	23.8680	23.6784
0.0	II	74.2966	56.6881	51.5395	49.9160	49.2587	48.8673
	III	74.2966	56.6881	51.5395	49.9160	49.2587	48.8673
	I	36.5161	26.8557	23.6396	22.5432	22.1145	21.8989
0.1	II	75.3618	55.4247	48.7874	46.5246	45.6399	45.1948
	III	75.3618	55.4247	48.7874	46.5246	45.6399	45.1948
	I	37.1294	25.9757	21.5323	19.7642	19.0224	18.6812
0.2	II	76.6274	53.6085	44.4383	40.7894	39.2584	38.5541
	III	76.6274	53.6085	44.4383	40.7894	39.2584	38.5541
	I	37.8703	24.6357	17.7314	13.9085	11.6641	10.2931
0.3	II	78.1565	50.8431	36.5941	28.7044	24.0724	21.2429
	III	78.1565	50.8431	36.5941	28.7044	24.0724	21.2429
				$\mu=2.0$			
	I	98.4856	75.1444	68.3194	66.1674	65.2961	64.7773
0.0	II	127.4670	97.2574	88.4241	85.6387	84.5110	83.8396
	III	182.6360	139.3510	126.6940	122.7030	121.0870	120.1250
	I	99.8976	73.4696	64.6713	61.6719	60.4991	59.9091
0.1	II	129.2950	95.0897	83.7024	79.8203	78.3024	77.5388
	III	185.2550	136.2450	119.9290	114.3660	112.1910	111.0970
	I	101.5750	71.0620	58.9063	54.0694	52.0399	51.1064
0.2	II	131.4660	91.9737	76.2409	69.9806	67.3539	66.1457
	III	188.3660	131.7800	109.2380	100.2680	96.5038	94.7726
	I	103.6020	67.3964	48.5082	38.0498	31.9098	28.1590
0.3	II	134.0900	87.2294	62.7829	49.2469	41.3000	36.4455
	III	192.1250	124.9820	89.9542	70.5587	59.1716	52.2155

Table 5. Proportionality factor $\sqrt{D^*_{eff} / \rho^*_{eff}}$ for simply-supported $(R_{1234} = 0)$ FG porous plate

Mode	μ	g	k	Ω	g	k	Ω	Proportionality factor	% change in Ω
I	0.5	0	0	12.3370	0	0.1	12.5139	1.0143	1.4
II				19.7395			20.0225	1.0143	1.4
III				32.4210			32.8858	1.0143	1.4
I					1		9.2033	0.7460	-25.4
II							14.7255	0.7460	-25.4
III							24.1858	0.7460	-25.4
I					2		8.1012	0.6567	-34.3
II							12.9620	0.6567	-34.3
III							21.2894	0.6567	-34.3
I					5		7.5046	0.6083	-39.2
II							12.0076	0.6083	-39.2
III							19.7217	0.6083	-39.2
I	1.0			19.7392	0	0.1	20.0222	1.0143	1.4
II				49.3480			50.0565	1.0143	1.4
III				49.3480			50.0565	1.0143	1.4
I					1		14.7253	0.7460	-25.4
II							36.8139	0.7460	-25.4
III							36.8139	0.7460	-25.4
I					2		12.9619	0.6567	-34.3
II							32.4053	0.6567	-34.3
III							32.4053	0.6567	-34.3
I					5		12.0074	0.6083	-39.2
II							30.0191	0.6083	-39.2
III							30.0191	0.6083	-39.2
I	2.0			49.3480	0	0.1	50.0556	1.0143	1.4
II				78.9579			80.0899	1.0143	1.4
III				128.3320			130.1720	1.0143	1.4
I					1		36.8132	0.7460	-25.4
II							58.9019	0.7460	-25.4
III							95.7344	0.7460	-25.4
I					2		32.4047	0.6567	-34.3
II							51.8482	0.6567	-34.3
III							84.2698	0.6567	-34.3
I					5		30.0185	0.6083	-39.2
II							48.0302	0.6083	-39.2
III							78.0645	0.6083	-39.2

Figure 2 shows the effect of the volume fraction index g on the first three values of the frequency parameter Ω for $k=0.2, \mu=2,$ $R_{1234}=1000$.

It is observed that frequency decreases with increasing value of g. This is due to the fact that a higher value of g introduces more metal components and reduces the stiffness of the plate, i.e., elasticity modulus and bending rigidity. The variation of non-dimensional frequency with porosity volume fraction k for $g=2, \mu=2, R_{1234}=1000$ is shown in Fig. 3.

The frequency decreases with increasing value of k. With the increase in k, the strength of the material decreases. It is concluded that even porosity distribution lowers the natural frequency.

The effect of aspect ratio μ on frequency for $k=0.2, g=2, R_{1234}=1000$ is shown in Fig. 4 and it is observed that frequency increases with increasing value of μ.

Fig. 5 demonstrates the frequency-response variation with R_{1234} for $k=0.2, \mu=2, g=2$. The frequency first increases and then becomes constant.

The variation of $\frac{z_0}{h}$, i.e., the distance between the physical neutral surface and the geometrical mid-plane with porosity volume fraction k for different values of volume fraction index g is shown in Fig. 6.

The value of $\frac{z_0}{h}$ increases with the increase in k. It is also observed that the value of $\frac{z_0}{h}$ for $g=5$ remains lower than that for $g=3$ up to k=0.09 and remains higher for k >0.09.

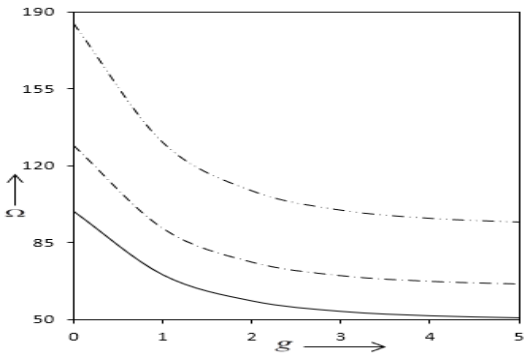

Fig. 2. Frequency parameter Ω of isotropic FG porous plate for $k=0.2, \mu=2, R_{1234}=1000$: First mode ——, Second mode –·–·–·–, Third mode–··–··

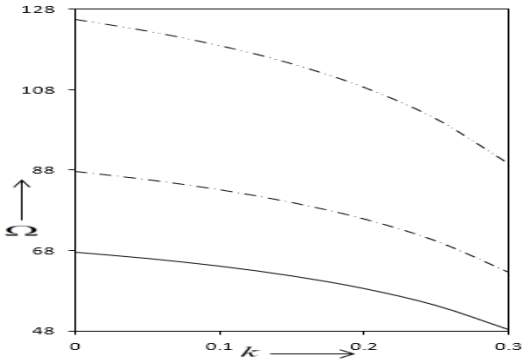

Fig. 3. Frequency parameter Ω of isotropic FG porous plate for $g=2, \mu=2, R_{1234}=1000$: First mode ——, Second mode –·–·–·–, Third mode –··–··

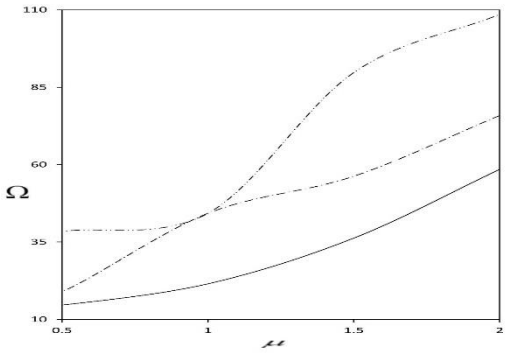

Fig. 4. Frequency parameter Ω of isotropic FG porous plate for $k=0.2, g=2, R_{1234}=1000$: First mode ——, Second mode –·–·–·–, Third mode –··–··

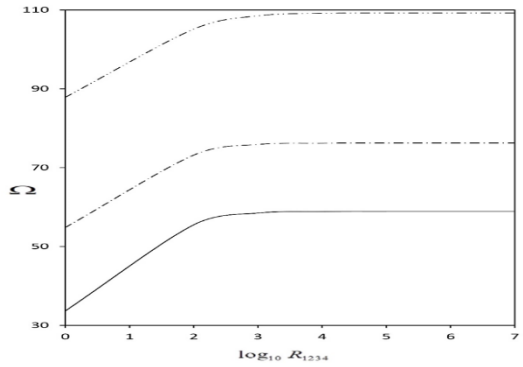

Fig. 5 Frequency parameter Ω of isotropic FG porous plate $k=0.2, \mu=2, g=2$: First mode ——, Second mode –·–·–·– , Third mode –··–··

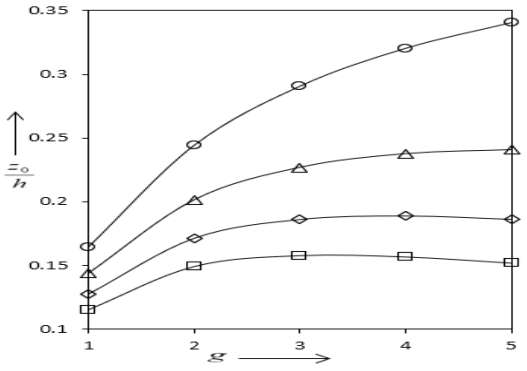

Fig. 6 Variation of z_0/h with volume fraction index g for different values of porosity volume fraction k; k=0 (□), k=0.1 (◊), k=0.2 (Δ), k=0.3 (O)

The value of z_0/h for $g=5$ remains lower than that for $g=4$ up to $k=0.16$ and remains higher for k>0.16. Variation of proportionality factor with g is shown in Fig. 7.

The first three mode shapes for FG porous square plate are shown in Fig. 8.

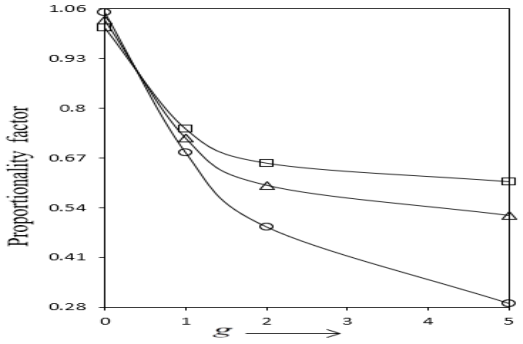

Fig. 7 Variation of proportionality factor with g for simply-supported FG porous plate without restraint edges for k=0.1 (□), k=0.2 (Δ), k=0.3 (O)

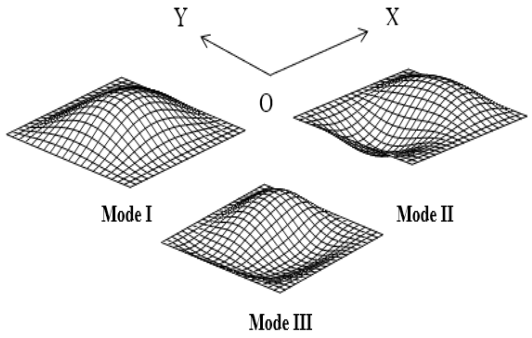

Fig. 8 First three mode shapes for FG porous square plate for $R_{12}=100, k=0.3, g=1$

4. Conclusion

Free transverse vibration of a thin isotropic FG rectangular porous plate is studied here. A simply-supported plate having all the edges elastically restrained against rotation is considered. Material properties are assumed to be graded in the thickness direction and are dependent on even porosity distribution. The first three frequencies are obtained using the Rayleigh-Ritz method and boundary characteristic orthogonal polynomials. The effects of volume fraction index, porosity volume index, aspect ratio, and restraint parameters are studied on the frequencies. It is concluded that

(i) The present technique is simple, straightforward forward, and provides good accuracy. The use of orthonormal polynomials results in a standard eigenvalue problem which can be easily solved for frequency parameters.

(ii) The frequency of porous plate is lower than that of FG plate.

(iii) Frequency generally decreases with increasing value of porosity volume fraction k. But, the variation of frequency with porosity volume fraction k is not monotonic for all the three modes as can be seen for $g=1, \mu=0.5, R_{1234}=100$. Here, frequencies in first and second modes decrease continuously but frequency in third mode first increases up to $k=0.1$ and then decreases. The porosity has a considerable effect on frequency in the case of thin plates.

(iv) The frequencies of isotropic simply-supported FG porous plate are proportional to those of simply-supported homogeneous isotopic plate and the proportionality factor is independent of the aspect ratio μ.

The results presented here may serve as a benchmark for further studies dealing with FG porous rectangular plates with elastically restrained edges.

Nomenclature

a	Length of the plate
b	Breadth of the plate
g	Volume fraction index
h	Thickness of the plate
k	Porosity volume fraction
t	Time
w	Displacement
N	Order of approximation
V, T	Strain and kinetic energies of the plate
$E(z)$	Young's modulus
E_m	Young's modulus of metal
E_c	Young's modulus of ceramic
r_1, r_2, r_3, r_4	Rotational spring constants
$V_{\max}, T_{\max}$	Maximum strain and kinetic energies of the plate
$U_{\max}$	Maximum strain energy associated to the rotational restraints
$\overline{W}$	Maximum transverse displacement
$\rho(z)$	Density of the plate material
υ	Poisson's ratio
Ω	Frequency parameter
μ	Aspect ratio
ω	Circular frequency
ρ_m	Density of metal
ρ_c	Density of ceramic

z_0	Distance between the geometrical mid-plane and the physical neutral surface
$\varepsilon_x, \varepsilon_y, \varepsilon_{xy}$	Normal and shear strains
$\sigma_x, \sigma_y, \sigma_{xy}$	Normal and shear stresses
ϕ_j	j[th] Orthogonal polynomial
$\hat{\phi}_j$	j[th] Orthonormal polynomial
δ_{ij}	The Kronecker delta

Acknowledgments

The author is thankful to the learned reviewers for their constructive comments.

Conflicts of Interest

The author declares that there is no conflict of interest regarding the publication of this manuscript.

References

[1] Yang, J., Shen, H.S., 2001. Dynamic response of initially stressed functionally graded rectangular thin plates. *Composite Structures*, 54, pp.497-508.

[2] Abrate, S., 2006. Free vibration, buckling, and static deflections of functionally graded plates. *Composite Science and Technology*, 66, pp.2383-2394.

[3] Ferreira, A.J.M., Batra, R.C., Roque, C.M.C., Qian L.F., Jorge, R.M.N., 2006, Natural frequencies of functionally graded plates by a meshless method. *Composite Structures*, 75, pp.593-600.

[4] Zhao, X., Lee, Y.Y., Liew, K.M., 2009. Mechanical and thermal buckling analysis of functionally graded plates. *Composite Structures*, 90, pp.161-171.

[5] Talha, M., Singh, B.N., 2010. Static response and free vibration analysis of FGM plates using higher order shear deformation theory. *Applied Mathematical Modelling*, 34, pp.3991-4011.

[6] Janghorban, M., Zareb, A., 2011. Thermal effect on free vibration analysis of functionally graded arbitrary straight-sided plates with different cutouts. *Latin American Journal of Solids and Structures*, 8, pp.245-257.

[7] Ghannadpour, S.A.M., Ovesy, H.R., Nassirnia, M., 2012. Buckling analysis of functionally graded plates under thermal loadings using finite strip method. *Computers and Structures*, 108-109, pp.93-99.

[8] Jaberzadeh, E., Azhari, M., Boroomand, B., 2013. Thermal buckling of functionally graded skew and trapezoidal plates with different boundary conditions using the element-free Galerkin method. *European Journal of Mechanics A/Solids*, 42, pp.18-26.

[9] Hasani Baferani, A., Saidi A.R., Ehtesham, H., 2013. On free vibration of functionally graded Mindlin plate and effect of in plane displacements. *Journal of Mechanics*, 29(2), pp.373- 384.

[10] Chakraverty, S., Pradhan, K.K., 2014. Free vibration of functionally graded thin rectangular plates resting on Winkler foundation with general boundary conditions using Rayleigh-Ritz method. *International Journal of Applied Mechanics*, 6(4), DOI: 10.1142/S1758825114500434.

[11] Chakraverty, S., Pradhan, K.K., 2014. Free vibration of exponential functionally graded rectangular plates in thermal environment with general boundary conditions. *Aerospace Science and Technology*, 36, pp.132-156.

[12] Pradhan, K.K., Chakraverty, S., 2015. Static analysis of functionally graded thin rectangular plates with various boundary conditions. *Archive of Civil and Mechanical Engineering*, 15(3), pp.721-734.

[13] Khorshidi, K., Bakhsheshy, A., 2015. Free vibration analysis of a functionally graded rectangular plate in contact with a bounded fluid. *Acta Mechanica*, 226(10), pp.3401-3423.

[14] Pham, T.T., 2016. Analytical solution for thermal buckling analysis of rectangular plates with functionally graded coatings. *Aerospace Science and Technology*, 55, pp.465-473.

[15] Atmane, H.A., Bedia, E.A.A., Bouazza, M., Tounsi, A., Fekrar, A., 2016. On the thermal buckling of simply supported rectangular plates made of a sigmoid functionally graded Al/Al2O3 based material. *Mechanics of Solids*, 51(2), pp.177-187.

[16] Young-Hoon Li, Seok-In, B., Ji-Hwan, K., 2016. Thermal buckling behavior of functionally graded plates based on neutral surface. *Composite Structures*, 137, pp.208-214.

[17] Kumar, S., Ranjan, V., Jan, P., 2018. Free vibration analysis of thin functionally graded rectangular plates using the dynamic stiffness method. *Composite Structures*, 197, pp.39-53.

[18] Porous Materials, http://www.uio.no/studier/emner/matnat/kjemi/KJM5100/h06/undervisningsmateriale/16KJM5100 2006 porous e.pdf.

[19] Theodorakopoulos, D.D., Beskos, D.E., 1994. Flexural vibration of poroelastic plates. *Acta Mechanica*, 103, pp.191-203.

[20] Leclaire, P., Cummings, A., Horoshenkov, K.V., 2001. Transverse vibration of a thin rectangular porous plate saturated by a fluid. *Journal of Sound and Vibration*, 247, pp.1-18.

[21] Leclaire, P., Horoshenkov, K.V., Swift, M.J., Hothersall, D.C., 2001. The vibrational response of a clamped rectangular porous plate. *Journal of Sound and Vibration*, 247, pp.19-31.

[22] Wattanasakulpong, N., Ungbhakorn, V., 2014. Linear and nonlinear vibration analysis of elastically restrained ends FGM beams with porosities. *Aerospace Science and Technology*, 32(1), pp.111-120.

[23] Rezaei, A., Saidi, A., 2015. Exact solution for free vibration of thick rectangular plates made of porous materials. *Composite Structures*, 134, pp.1051-1060.

[24] Mojahedin, A., Jabbari, M., Khorshidvand, A., Eslami, M., 2016. Buckling analysis of functionally graded circular plates made of saturated porous materials based on higher order shear deformation theory. *Thin-Walled Structures*, 99, pp.83-90.

[25] Chen, D., Yang, J., Kitipornchai, S., 2016. Free and forced vibrations of shear deformable functionally graded porous beams. *International Journal of Mechanical Sciences*, 108, pp.14-22.

[26] Ebrahimi, F., Habibi, S., 2016. Deflection and vibration analysis of higher-order shear deformable compositionally graded porous plate. *Steel and Composite Structures*, 20(1), pp.205-225.

[27] Mechab, I., Mechab, B., Benaissa, S., Serier, B., Bouiadjra, B.B., 2016. Free vibration analysis of FGM nanoplate with porosities resting on Winkler Pasternak elastic foundations based on two-variable refined plate theories. *Journal of the Brazilian Society of Mechanical Sciences and Engineering*, 38(8), pp.2193-2211.

[28] Mechab, B., Mechab, I., Benaissa, S., Ameri, M., Serier, B., 2016. Probabilistic analysis of effect of the porosities in functionally graded material nanoplate resting on Winkler-Pasternak elastic foundations. *Applied Mathematical Modelling*, 40(2), pp.738-749.

[29] Jahwari, A.F., Naguib, H.E., 2016. Analysis and homogenization of functionally graded viscoelastic porous structures with a higher order plate theory and statistical based model of cellular distribution. *Applied Mathematical Modelling*, 40(3), pp.2190-2205.

[30] Barati, M.R., Sadr, M.H., Zenkour, A.M., 2016. Buckling analysis of higher order graded smart piezoelectric plates with porosities resting on elastic foundation. International *Journal of Mechanical Sciences*, 117, pp.307-320.

[31] Barati, M. R., Zenkour, A. M., 2016. Electro-thermoelastic vibration of plates made of porous functionally graded piezoelectric materials under various boundary conditions. *Journal of Vibration and Control*, 24(10), pp.1910-1926.

[32] Mouaici, F., Benyoucef, S., Atmane, H.A., Tounsi, A., 2016. Effect of porosity on vibrational characteristics of non-homogeneous plates using hyperbolic shear deformation theory. *Wind Structures*, 22, pp.429-454.

[33] Ebrahimi, F., Jafari, A., 2016. Buckling behavior of smart EEE-FG porous plate with various boundary conditions based on refined theory. *Advances in Material Research*, 5(4), pp.279-298.

[34] Rezaei, A.S., Saidi, A.R., 2015. Exact solution for free vibration of thick rectangular plates made of porous materials. *Composite Structures*, 134, pp.1051-1060.

[35] Rezaei, A.S., Saidi, A.R., 2016. Application of Carrera unified formulation to study the effect of porosity on natural frequencies of thick porous-cellular plates. *Composites Part B: Engineering*, 91, pp.361-370.

[36] Rezaei, A.S., Saidi, A.R., Abrishamdari, M., Mohammadi, M.H.P., 2017. Natural frequencies of functionally graded plates with porosities via a simple four variable plate theory: An analytical approach. *Thin-Walled Structures*, 120, pp.366-377.

[37] Rezaei, A.S., Saidi, A.R., 2017. On the effect of coupled solid-fluid deformation on natural frequencies of fluid saturated porous plates. *European Journal of Mechanics – A/Solids*, 63, pp.99-109.

[38] Rezaei, A.S., Saidi, A.R., 2017. Buckling response of moderately thick fluid-infiltrated porous annular sector plates. *Acta Mechanica*, 228(11), pp.3929-3945.

[39] Rezaei, A.S., Saidi, A.R., 2017. An analytical study on the free vibration of moderately thick fluid-infiltrated porous annular sector plates. *Journal of Vibration and Control*, 24(18), pp.4130-4144.

[40] Askari, M., Saidi, A.R., Rezaei, A.S., 2017. On natural frequencies of Levy-type thick porous cellular plates surrounded by piezoelectric layers. *Composite Structures*, 179, pp.340-354.

[41] Kamranfard, M.R., Saidi, A.R., Naderi, A., 2017. Analytical solution for vibration and buckling of annular sectorial porous plates under in-plane uniform compressive loading. *Proceedings of the Institution of Mechanical Engineering Part C: Journal of Mechanical Engineering Sciences*, 232(12), pp.2211-2228.

[42] Şimşek, M., Aydın, M., 2017. Size-dependent forced vibration of an imperfect functionally

graded (FG) microplate with porosities subjected to a moving load using the modified couple stress theory. *Composite Structures*, 160, pp.408-421.

[43] Akbaş, Ş.D., 2017. Vibration and static analysis of functionally graded porous plates. *Journal of Applied and Computational Mechanics*, 3(3), pp.199-207.

[44] Ebrahimi, F., Jafari, A., Barati, M.R., 2017. Vibration analysis of magneto-electro-elastic heterogeneous porous material plates resting on elastic foundations. *Thin-Walled Structures*, 119, pp.33-46.

[45] Shahverdi, H., Barati, M.R., 2017. Vibration analysis of porous functionally graded nanoplates. *International Journal of Engineering Sciences*, 120, pp.82-99.

[46] Barati, M.R., Shahverdi, H., Zenkour, A.M., 2017. Electro-mechanical vibration of smart piezoelectric FG plates with porosities according to a refined four-variable theory. *Mechanics of Advanced Materials and Structures*, 24(12), pp.987-998.

[47] Ebrahimi, F., Jafari, A., Barati, M.R., 2017, Free vibration analysis of smart porous plates subjected to various physical fields considering neutral surface position. *Arabian Journal for Science and Engineering*, 42(5), pp.1865-1881.

[48] Ali, G.A., Zahra, K.M., Mehdi, K., Iman, A., 2017. Free vibration of embedded porous plate using third-order shear deformation and poroelasticity theories. *Journal of Engineering*, pp.1-13, DOI: 10.1155/2017/1474916.

[49] Wang, Y.Q., Zu, J.W., 2017. Vibration behaviors of functionally graded rectangular plates with porosities and moving in thermal environment. *Aerospace Science and Technology*, 69, pp.550-562.

[50] Wang, Y.Q., Zu, J.W., 2017. Large-amplitude vibration of sigmoid functionally graded thin plates with porosities. *Thin-Walled Structures*, 119, pp.911-924.

[51] Wang, Y.Q., Zu, J.W., 2017. Porosity-dependent nonlinear forced vibration analysis of functionally graded piezoelectric smart material plates. *Smart Materials and Structures*, 26(10), pp.105014.

[52] Wang, Y.Q., Yang, Z., 2017. Nonlinear vibrations of moving functionally graded plates containing porosities and contacting with liquid: internal resonance. *Nonlinear Dynamics*, 90(2), pp.1461-1480.

[53] Wang, Y.Q., 2018. Electro-mechanical vibration analysis of functionally graded piezoelectric porous plates in the translation state. *Acta Astronautica*, 143, pp.263-271.

[54] Kiran, M.C., Kattimani, S.C., Vinyas, M., 2018. Porosity influence on structural behavior of skew functionally graded magneto-electro-elastic plate. *Composite Structures*, 191, pp.36-77.

[55] Arshid, E., Khorshidvand, A. R., 2018. Free vibration analysis of saturated porous FG circular plates integrated with piezoelectric actuators via differential quadrature method. *Thin-Walled Structures*, 125, pp.220-233.

[56] Arani, A.G., Khani, M., Maraghi, Z.K., 2018. Dynamic analysis of a rectangular porous plate resting on an elastic foundation using high-order shear deformation theory. *Journal of Vibration and Control*, 24, pp.3698-3713.

[57] Gupta, A., Talha, M., 2018. Influence of porosity on the flexural and free vibration responses of functionally graded plates in thermal environment. *International Journal of Structural Stability and Dynamics*, 18 (1), DOI:10.1142/S021945541850013X.

[58] Zhao, J., Wang, Q., Deng, X., Choe, K., Zhong, R., Shuai, C., 2019. Free vibrations of functionally graded porous rectangular plate with uniform elastic boundary conditions. *Composites Part B: Engineering*, 168, pp.106-120.

[59] Daikh, A.A., Zenkour, A. M., 2019. Free vibration and buckling of porous power-law and sigmoid functionally graded sandwich plates using a simple higher-order shear deformation theory. *Material Research Express*, 6, DOI: 10.1088/2053-1591/ab48a9.

[60] Du, Y., Wang, S., Sun, L., Shan, Y., 2019. Free vibration of rectangular plates with porosity distributions under complex boundary constraints. *Shock and Vibration*, DOI: 10.1155/2019/6407174.

[61] Al Rjoub, Y. S., Alshatnawi, J.A., 2020. Free vibration of functionally-graded porous cracked plates. *Structures*, 28, pp.2392-2403.

[62] Bansal, G., Gupta, A., Katiyar, V., 2020. Vibration of porous functionally graded plates with geometric discontinuities and partial supports. *Proceedings of the Institution of Mechanical Engineers Part C: Journal of Mechanical Engineering Science*, 234(21), pp.4149-4170.

[63] Tran, T.T., Quoc-Hoa Pham, 2021. Static and free vibration analyses of functionally graded porous variable-thickness plates using an edge-based smoothed finite element method. *Defence Technology*, 17(3), pp.971-986.

[64] Chai, Q., & Wang, Y.Q., 2022. Traveling wave vibration of grapheme platelet reinforced porous joined conical-cylindrical shells in a spinning motion. *Engineering Structures*, 252(1), DOI: 10.1016/ j.engstruct.2021.113718.

[65] Kumar, Y., 2018. The Rayleigh-Ritz method for linear dynamic, static and buckling behavior of beams, shells and plates: A literature review. *Journal of Vibration and Control*, 24(7), pp.1205-1227.

[66] Pablo, M.G., Jose, V.A.S., Harmani, L., 2017. A review and study on Ritz method admissible functions with emphasis on buckling and free vibration of isotropic and anisotropic beams and plates. *Archive of Computational Methods in Engineering*, 25(3), pp.785-815.

[67] Wang, Y.Q., Zu, J.W., 2017. Analytical analysis for vibration of longitudinally moving plate submerged in infinite liquid domain. *Applied Mathematics and Mechanics*, 38(5), pp.625-646.

[68] Wang, Y.Q., Ye, C., Zu, J.W., 2018. Identifying the temperature effect on the vibrations of functionally graded cylindrical shells with porosities. *Applied Mathematics and Mechanics*, 39(11), pp.1587-1604.

[69] Laura, P.A.A., & Grossi, R., 1979. Transverse vibrations of rectangular anisotropic plates with edges elastically restrained against rotation. *Journal of Sound and Vibration*, 64(2), pp.257-267.

[70] Okan, M.B., 1982. Free and damped vibrations of an orthotropic rectangular plate with one edge free while the rest are elastically restrained against rotation. *Ocean Engineering*, 9(2), pp.127-134.

[71] Kumar, Y., 2012. Free vibrations of simply supported nonhomogeneous isotropic rectangular plates of bilinearly varying thickness and elastically restrained edges against rotation using Rayleigh-Ritz method. *Earthquake Engineering and Engineering Vibration*, 11(2), DOI: 10.1007/s11803-012-0117-1.

[72] Zhang, Y., & Zhang, S., 2019. Free transverse vibration of rectangular orthotropic plates with two opposite edges rotationally restrained and remaining others free. *Applied Sciences*, 9, DOI: 10.3390/app9010022.

[73] He, Y., Duan, M., & Su, J., 2021. Bending of rectangular orthotropic plates with rotationally restrained and free edges: Generalized integral transform solutions. *Engineering Structures*, 247, DOI: 10.1016/j.engstruct.2021.113129.

[74] Warburton, G.B., Edney, S.L., 1984. Vibrations of rectangular plates with elastically restrained edges. *Journal of Sound and Vibration*, 95(4), pp.537-552.

[75] Singh, B., Chakraverty, S., 1994. Flexural vibration of skew plates using boundary characteristic orthogonal polynomials in two variables. *Journal of Sound and Vibration*, 173(2), pp.157-178.

[76] Leissa, A.W., 1973. The free vibration of rectangular plates. *Journal of Sound and Vibration*, 31(3), pp.257-293.